THE JOURNAL OF BIOLOGICAL CHEMISTRY VOL. 289, NO. 21, pp. 15130–15140, May 23, 2014


# An Internally Modulated, Thermostable, pH-sensitive Cys Loop Receptor from the Hydrothermal Vent Worm *Alvinella pompejana*[*] [S]

Received for publication, October 8, 2013, and in revised form, April 4, 2014 Published, JBC Papers in Press, April 9, 2014, DOI 10.1074/jbc.M113.525576

**Puneet Juneja[‡], Reinhold Horlacher[§], Daniel Bertrand[¶], Ryoko Krause[¶], Fabrice Marger[¶], and Wolfram Welte[‡1]**

*From the [‡]Fachbereich Biologie, Universität Konstanz, Universitätsstraße 10, 78457 Konstanz, Germany, [§]Trenzyme, Byk-Gulden-Straße 2, 78467 Konstanz, Germany, and [¶]HiQScreen Sàrl, 6, rte. de Compois, 1222 Vésenaz, Geneva, Switzerland*

**Background:** Cys loop receptors from the hydrothermal vent worm *Alvinella pompejana* were studied.
**Results:** A Cys loop receptor opens at low pH, is chloride-specific, is modulated by its N-terminal extension, and is modestly thermostable.
**Conclusion:** Cys loop receptors from worms living in extreme and secluded habitats are more closely related to eukaryotic than to prokaryotic family members.
**Significance:** We studied the first known Cys loop receptor from a hydrothermal vent worm.

**Cys loop receptors (CLRs) are commonly known as ligand-gated channels that transiently open upon binding of neurotransmitters to modify the membrane potential. However, a class of cation-selective bacterial homologues of CLRs have been found to open upon a sudden pH drop, suggesting further ligands and more functions of the homologues in prokaryotes. Here we report an anion-selective CLR from the hydrothermal vent annelid worm *Alvinella pompejana* that opens at low pH. *A. pompejana* expressed sequence tag databases were explored by us, and two full-length CLR sequences were identified, synthesized, cloned, expressed in *Xenopus* oocytes, and studied by two-electrode voltage clamp. One channel, named Alv-a1-pHCl, yielded functional receptors and opened upon a sudden pH drop but not by other known agonists. Sequence comparison showed that both CLR proteins share conserved characteristics with eukaryotic CLRs, such as an N-terminal helix, a cysteine loop motif, and an intracellular loop intermediate in length between the long loops of other eukaryotic CLRs and those of prokaryotic CLRs. Both full-length Alv-a1-pHCl and a truncated form, termed tAlv-a1-pHCl, lacking 37 amino-terminal residues that precede the N-terminal helix, formed functional channels in oocytes. After pH activation, tAlv-a1-pHCl showed desensitization and was not modulated by ivermectin. In contrast, pH-activated, full-length Alv-a1-pHCl showed a marked rebound current and was modulated significantly by ivermectin. A thermostability assay indicated that purified tAlv-a1-pHCl expressed in Sf9 cells denatured at a higher temperature than the nicotinic acetylcholine receptor from *Torpedo californica*.**

The best known CLR[2] superfamily members are homo- or heteropentameric membrane proteins that form transient ion channels upon binding of small ligands (neurotransmitters) such as acetylcholine, glycine, glutamate, GABA, serotonin, and histamine (1). As a subclass of the ligand-gated ion channels, they are also named pentameric ligand-gated channels. The channel opening or activation allows the passage of ions such as $Na^+$, $K^+$, $Ca^{2+}$, and $Cl^-$, and the resulting membrane polarization causes activation or inhibition of the postsynaptic membrane (2–4).

The CLR superfamily shares a common domain architecture with an N-terminal helix and an extracellular ligand-binding domain (LBD), followed by four transmembrane helices designated M1, M2, M3, and M4. The cytoplasmic part (CP) is of variable size, mainly formed by a linker between the M3-M4 helices comprising between six (prokaryotic CLRs) and 250 (neuronal CLRs) amino acids. The binding sites for agonists (transmitters) and competitive inhibitors are in the interfaces between the five subunits (2, 5). The prokaryotic homologues (6) also share this architecture but have a low sequence similarity with their eukaryotic counterparts. GLIC for instance shares 20% sequence identity with the human α7 nicotinic acetylcholine receptor (nAChR)) and is made up of a smaller number of residues (7). This is mainly due to the absence of the N-terminal helix and a much shorter M3-M4 linker (8). Functionally, GLIC does not respond to an agonist but is activated by low pH (protons) and is cation-selective (7).

Here we describe the identification and characterization of a pH-activated eukaryotic CLR from a thermophilic polychaete annelid, *Alvinella pompejana* (9). This worm was first discovered in 1980. It exclusively colonizes deep-sea hydrothermal vents and is believed to be one of the most heat-tolerant animals. Its ability to survive under extreme conditions, such as

* This work was supported by EU grant 202088 (Neurocypres) and by the Konstanz Research School of Chemical Biology (KoRS-CB).
[S] This article contains supplemental Figs. 1–4.
[1] To whom correspondence should be addressed: Fachbereich Biologie, Universität Konstanz, Universitätsstr. 10, 78457 Konstanz, Germany. Tel.: 49-7531-88-2206; Fax: 49-7531-88-3183; E-mail: wolfram.welte@uni-konstanz.de.

[2] The abbreviations used are: CLR, Cys loop receptor; LBD, ligand binding domain; CP, cytoplasmic part; DDM, *n*-dodecyl-β-D-maltopyranoside; nAChR, nicotinic-acetylcholine receptor; PB, phenobarbitone; ACh, acetylcholine; EST, expressed sequence tag.

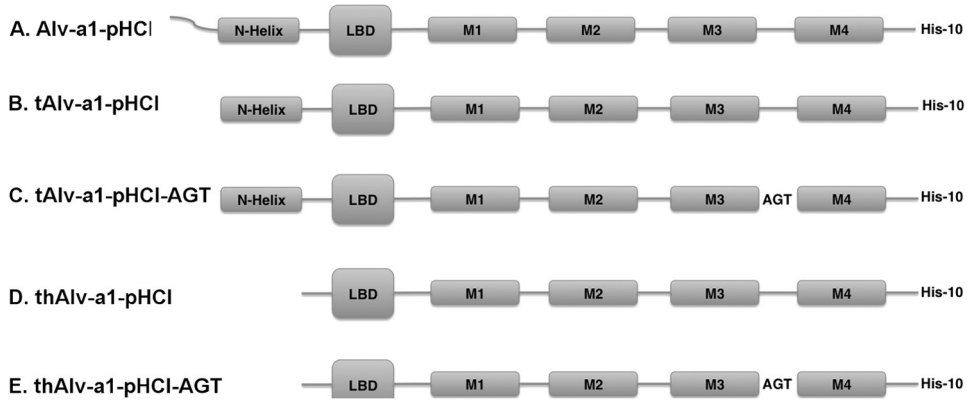


FIGURE 1. **Different expression constructs of Alv-a1-phCl.** Alv-a1-pHCl has an N-terminal extension of 37 residues (supplemental Fig. 1*A*) followed by the N-terminal helix and the LBD. The transmembrane part is formed by the transmembrane helices M1-M4. *A*, Alv-a1-pHCl full-length protein. *B*, tAlv-a1-phCl lacks 37 N-terminal residues that likely are disordered. *C*, tAlv-a1-phCl-AGT. The M3-M4 loop is replaced by the tripeptide AGT. *D*, thAlv-a1-pHCl, N-terminally truncated by the 37 N-terminal residues and the N-terminal helix. *E*, thAlv-a1-pHCl-AGT, as the latter, but with the M3-M4 helix replaced by the tripeptide AGT. The constructs in *A–C* were used for oocyte experiments, and the constructs in *B–E* were used for Sf9 expression.

low pH, high concentration of heavy metals, sulfides, and temperatures up to 80 °C (10, 11), makes it a suitable candidate for studying adaptation, evolution, and thermostabilization of eukaryotic proteins and may be suitable for biophysical and structural work.

## EXPERIMENTAL PROCEDURES

*Sequence Determination*—EST sequences of CLRs were found by bioinformatic procedures in the *A. pompejana* EST sequence database at NCBI and the *A. pompejana* cDNA sequences database (12). Gene reconstruction from EST sequences was done with ClustalW, available at the European Bioinformatics Institute. Phylogenetic analysis was done using the phylogenesis server at Phylogeny.fr (13).

*Gene and Plasmid Construction*—The reconstructed coding sequence of Alv-a1-pHCl was translated into the corresponding amino acid sequence. For all expression constructs of the Alv-a1-pHCl protein, the native signal sequence was replaced by the rat $GABA_A$ β3 receptor signal sequence prior to codon optimization and gene synthesis. A C-terminal $His_{10}$ tag and flanking restriction sites for further cloning were added at this step. Five constructs of Alv-a1-pHCl were made by fusion PCR and/or partial gene synthesis: a full-length protein gene construct (Alv-a1-pHCl), a truncated protein gene construct lacking the 37 N-terminal disordered amino acids according to secondary structure prediction (tAlv-a1-pHCl), a further truncated gene construct also lacking the N-terminal helix (thAlv-a1-pHCl), and mutants of the latter two with the M3-M4 sequence (KAMKAKKAGQPASKVAGAEDGQDE) replaced by the tripeptide AGT (tAlv-a1-pHCl-AGT and thAlv-a1-pHCl-AGT) (Fig. 1 and supplemental Fig. 1*A*). Alv-a9 was expressed as full-length protein with its native signal sequence. For expression in oocytes, DNA was subcloned in the pcDNA 3.1+ vector. For expression in Sf9 cells, DNA was subcloned in the pVL1393 vector.

*Sf9 Expression and Purification*—The flashBAC GOLD expression system (Oxford Expression Technologies) was used for the construction of recombinant virus from the pVL1393 vector. Recombinant viruses were generated for the tAlv-a1-pHCl, tAlv-a1-pHCl-AGT, thAlv-a1-pHCl, and thAlv-a1-pHCl-AGT constructs. Whole cells were suspended in 10 mM Tris, 1 mM EDTA (pH 7.5) with protease inhibitor (Complete Ultra, Roche). Cells were lysed by nitrogen decompression or mechanical homogenization. The resulting homogenate was centrifuged at 1500 × g for 15 min to remove cell debris and unbroken cells, and the supernatant was centrifuged at 100,000 × g for 1 h to collect the membranes. Membranes were suspended in 20 mM Tris, 150 mM NaCl (pH 7.5), and expression was checked with Western blot analysis (anti-His tag antibody). For purification, receptor-containing membranes were solubilized with 1% *n*-dodecyl-β-D-maltopyranoside (DDM) for 1 h at 4 °C and centrifuged at 100,000 × g for 1 h in TNB (20 mM Tris, 150 mM NaCl, 20 mM imidazole, 0.03% DDM (pH 7.5)). The supernatant was passed over a nickel-Sepharose column equilibrated with TNB and eluted with modified TNB that contained 300 mM imidazole. All steps were performed on ice or at 4 °C.

*Thermostability Assay*—Nickel-Sepharose affinity-purified tAlv-a1-pHCl in TNB was incubated at 40, 50, 55, 65, and 70 °C for 10 min or at 50 °C for 20 min, and fractions were run on blue native PAGE (14).

The nicotinic acetylcholine receptor (nAChR) from *Torpedo californica* in complex with α-bungarotoxin was affinity-purified[3] in the presence of 0.05% Cymal6 in 100 mM sodium phosphate, 150 mM NaCl (pH 7.5). Samples were incubated at 25 and 50 °C for 10 min and analyzed by blue native PAGE as above.

*Expression of Alv-a1-pHCl, tAlv-a1-pHCl, and tAlv-a1-pHCl-AGT in Xenopus Oocytes*—*Xenopus* oocytes were prepared using standard procedures (15), and an automated injection device was used for cDNA injection (RoboInject, Multichannel Systems, Germany) (16). Briefly, following the regulation of animal experimentation set by the canton of Geneva, Switzerland, ovaries were harvested from deeply anesthetized female *Xenopus laevis*. A small piece of ovary was isolated for immediate preparation, whereas the remaining piece was stored at 4 °C in a sterile Barth solution containing 96 mM NaCl, 1 mM KCl, 2.4 mM $NaHCO_3$, 10 mM HEPES, 0.82 mM

[3] P. Juneja and W. Welte, unpublished data.

$MgSO_4 \cdot 7H_2O$, 0.33 mM $Ca(NO_3)_2 \cdot 4H_2O$, and 0.41 mM $CaCl_2 \cdot 6H_2O$ (pH 7.4), and supplemented with 20 $\mu$g/ml of kanamycin, 100 unit/ml penicillin, and 100 $\mu$g/ml streptomycin. Two days after dissociation, oocytes were injected intranuclearly with 10 nl of solution, yielding a final amount of 0.2 ng of plasmid containing the cDNA of interest per oocyte.

*Voltage Clamp Experiments*—Between 2 and 7 days after injection, currents evoked were recorded using an automated platform equipped with a two-electrode voltage clamp (HiClamp, Multichannel Systems). All recordings were performed at 20 °C, and cells were superfused with modified OR2 medium containing 82.5 mM NaCl, 2.5 mM KCl, 5 mM HEPES, and 1.8 mM $CaCl_2 \cdot 2H_2O$ and adjusted to pH 7.4. HEPES was replaced with $KH_2PO_4$ for solutions with low pH. Cells were held at −80 mV. Data were filtered at 50 Hz, captured at 500 Hz, and analyzed offline. To obtain stable pH values between 2 and 4, solutions were buffered with 10 mM acetate buffer. The pH was adjusted by calculating the buffer components. The empirical Hill equation with either a single or dual component was used to fit concentration-activation curves. Single component concentration activation curves are in the form

$$Y = \frac{1}{\left[1 + \left(\frac{x}{EC_{50}}\right)^{n_H}\right]} \quad \text{(Eq. 1)}$$

where $Y$ is the fraction of evoked current, $EC_{50}$ is the concentration for 50% activation, and $n_H$ is the apparent cooperativity. Concentration-inhibition curves were also fitted with Hill equations in the form

$$Y = \frac{1}{\left[1 + \left(\frac{xIC_{50}}{x}\right)^{n_H}\right]} \quad \text{(Eq. 2)}$$

where $Y$ is the fraction of evoked current, $IC_{50}$ is the concentration for 50% inhibition, and $n_H$ is the apparent cooperativity. Data analysis and curve fitting were done using Matlab (Mathworks Inc.) or Excel (Microsoft).

## RESULTS

*Sequence Analysis*—To reconstruct the 5′-3′ code for the full-length Alv-a1-pHCl CLR, we used the following EST sequences: GO149973.1, GO164508.1, GO215979.1, GO215980.1, and TERA02171. The complementary code of GO215980.1 and the other EST sequences yielded a complete open reading frame coding for 443 residues (supplemental Fig. 2). For Alv-a9, the complete open reading frame was contained in TERA03200 and codes for 447 residues.

A multiple alignment of the Alv-a1-pHCl constructs and Alv-a9 with members of the CLR family is given in supplemental Fig. 1*A*. Alv-a1-pHCl shows 36% amino acid identity with the human glycine $\alpha$1 receptor. Alv-a9 shows 27.0% identity with the human nAChR $\alpha$9 subunit (Fig. 2, *A* and *B*). Both were predicted with individual signal sequences of 25 and 18 residues and an N-terminal helix followed by LBDs (Fig. 2), as is distinctive for eukaryotic CLRs. In the case of Alv-a1-pHCl, the N-terminal helix is preceded by a 37 amino acid long extension lacking apparent homology and secondary structure. Furthermore, a transmembrane domain of four transmembrane helices and a CP (Fig. 2) were predicted. The M3-M4 loops representing the largest part of the CP are comprised of 27 and 70 residues in Alv-a1-pHCl and Alv-a9, respectively, shorter than in most eukaryotic CLRs. Phylogenetic analysis puts Alv-a1-pHCl together with anion-selective CLRs and Alv-a9 with cation-selective CLRs, in accord with multiple sequence alignments (Fig. 3).

*Sf9 Expression and Purification*—tAlv-a1-pHCl, thAlv-a1-pHCl, tAlv-a1-pHCl-AGT, and thAlv-a1-pHCl-AGT were expressed in Sf9 cells, and membrane fractions were prepared. Western blot analyses with anti-His tag antibodies showed, in each case, two closely spaced bands with an apparent molecular mass near 37 kDa (supplemental Fig. 3), indicating that the receptor protein was targeted to the membranes.

In SDS-PAGE, two closely spaced bands were found at an apparent molecular mass of 37 kDa. To rule out the presence of truncated polypeptides, we performed mass spectrometric analysis by MALDI and Western blotting with anti-His tag antibodies for the tAlv-a1-pHCl construct. The presence of an N-terminal fragment and the staining of the C terminus with anti-His tag antibodies indicate the integrity of the protein (data not shown). The Alv-a9 sequence was not used for Sf9 expression.

*Thermostability*—Purified tAlv-a1-pHCl in TNB was incubated at different temperatures (at 40, 50, 55, and 65 °C for 10 min and at 50 °C for 20 min) and subjected to blue native PAGE (Fig. 4). A single band after 10 min of heat treatment at temperatures of 40, 50, and 55 °C and after 20 min of heat treatment at 50 °C was seen, whereas, at 65 °C, a weak band appeared at the same position. The result suggests that the protein denatures and precipitates at a temperature between 55 and 65 °C.

For comparison we purified the nAChR from *T. californica* in complex with $\alpha$-bungarotoxin using the detergent Cymal 6. When the receptor is kept at room temperature, it runs partly as a dimer and partly as a monomer (Fig. 4). After heating to 50 °C for 10 min, the bands are absent. This indicates that tAlv-a1-pHCl is at least 15 °C more thermostable than the nAChR from *T. californica*.

Comparison with proteins of known molecular mass on blue native PAGE shows (Fig. 4) that tAlv-a1-pHCl migrates at an apparent molecular mass in accord with the 235 kDa expected for the homopentamer. The *Torpedo* nAChR receptor migrates as two bands at apparent molecular masses expected for heteropentameric receptors and their dimers.

*Electrophysiological Studies and pH Activation*—When Alv-a1-pHCl and tAlv-a1-pHCl were expressed in *Xenopus* oocytes, a current could be evoked only after a change from neutral to low pH, whereas other well known neurotransmitters failed to evoke any response (Fig. 5, *A* and *B*). For the full-length Alv-a1-pHCl, an additional rebound current was observed (Figs. 5*B* and 10*A*), indicating that activation is potentiated in presence of the N-terminal 37 residues. The current did not return completely to its level before excitation (confirmed with four different oocytes).

Determination of the pH sensitivity of tAlv-a1-pHCl yielded a typical concentration activation curve with an $EC_{50}$ at pH

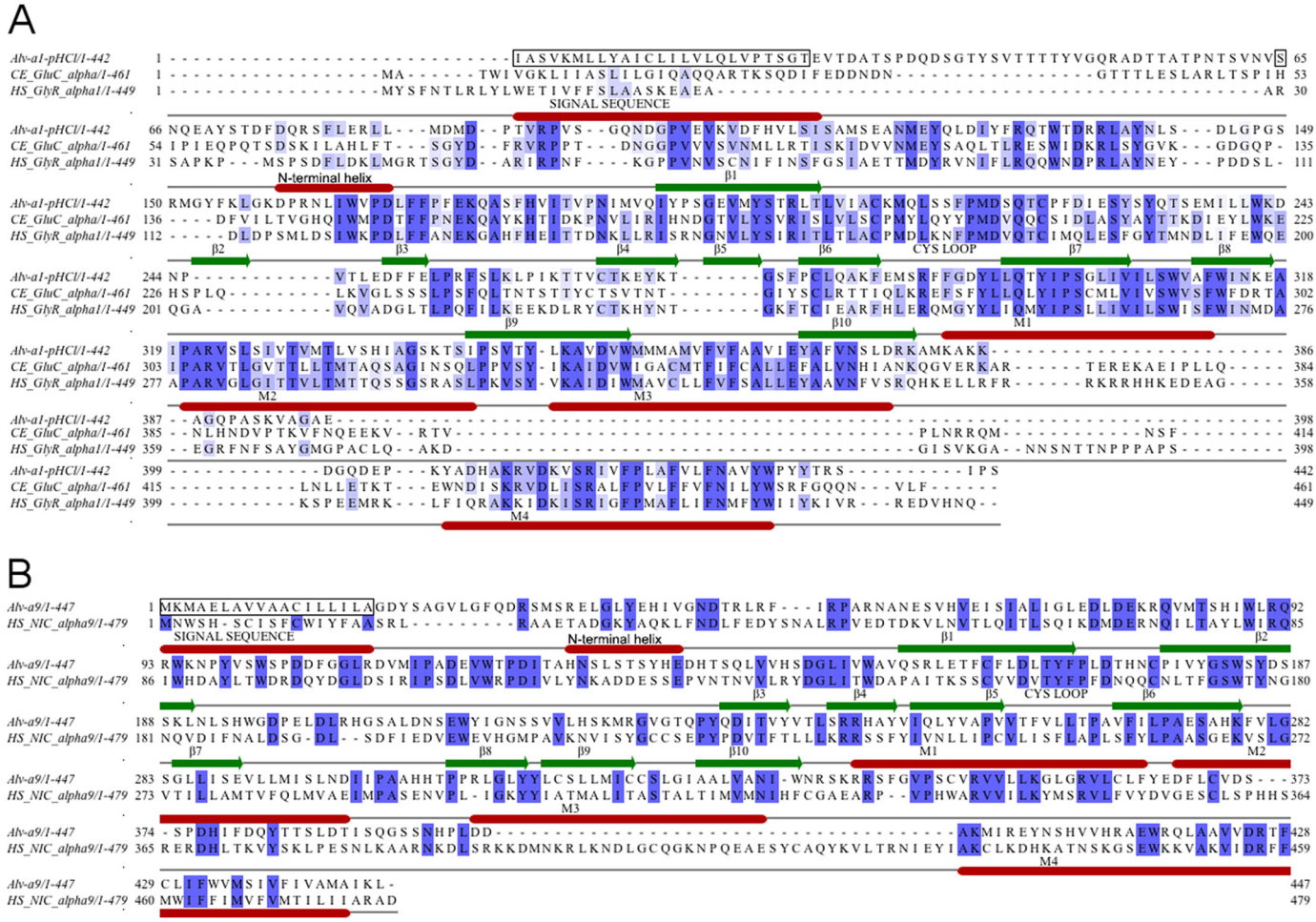


FIGURE 2. **Sequence alignments of Alv-a1-pHCl and Alv-a9 with their closest homologues.** Alignment of Alv-a1-pHCl with the glutamate-gated ion channel of *C. elegans* and human glycine $\alpha$1 (*A*) and Alv-a9 with the human $\alpha$9 sequence (*B*). The construct tAlv-a1-pHCl is N-terminally truncated before Ser-65 (*green*, *boxed*). The M3-M4 loop is marked in *pink*. Secondary structure elements are indicated by *bars*. An alignment with all members of the CLR family is given in supplemental Fig. 1*A*.

3.24. A fit with the Hill equation yielded a Hill coefficient of 2.55 (Fig. 6*C*).

We next determined the ionic selectivity of tAlv-a1-pHCl and found that it was permeable to chloride (Fig. 7). The construct tAlv-a1-pHCl-AGT lacking M3-M4 was inactive.

*Sensitivity to Picrotoxin and Other Antagonists*—Sensitivity of tAlv-a1-pHCl to various known blockers of chloride-permeable channels was examined. Exposure to fipronil, niflumic acid, lidocaine, bupivacaine hydrochloride, strychnine, tubocurarine chloride pentahydrate, tetramethylammonium chloride, tetracaine, mecamilamine, hexamethonium, and $\alpha$-endosulfan caused no inhibition of the pH-evoked current. Although lindane at 100 $\mu$M reduced the normalized current by 55%, this is weak compared with the nM IC50 values reported for invertebrate receptors (data not shown).

Partial inhibition (78%) was, however, observed when cells were incubated in the presence of the open channel blocker picrotoxin (Fig. 8). The $IC_{50}$ observed was 123 $\mu$M. For full-length Alv-a1-pHCl, we observed the same $IC_{50}$ (data not shown), indicating that sensitivity to picrotoxin is independent of the 37 N-terminal residues.

*Sensitivity to Ivermectin and PNU-120596*—Furthermore, the anthelmintic drug ivermectin, known for its broad spectrum of modulating actions on chloride-permeable receptors from invertebrates as well as cation-permeable channels such as P2X or $\alpha$7 nAChRs (17, 18), was examined. Exposure of tAlv-a1-pHCl to ivermectin caused no detectable modification of the pH-evoked current (Fig. 9), whereas full-length Alv-a1-pHCl showed strong modulation by ivermectin (Fig. 10). From its sequence similarity with other CLRs, it was predicted that this receptor might be modulated by the $\alpha$7 positive allosteric modulator PNU-120596 (19). However, PNU-120596 exerts no activity at the tAlv-a1-pHCl receptor (Fig. 9).

*Role of the M3-M4 Loop and the N-terminal Helix*—To investigate the role of the M3-M4 loop, we constructed tAlv-a1-pHCl-AGT, in which the M3-M4 loop (KAMKAKKAGQ-PASKVAGAEDGQDE) was replaced by the tripeptide AGT (20). When this construct was expressed in oocytes, no current could be evoked by a pH drop (data not shown).

thAlv-a1-pHCl lacking the N-terminal helix and thAlv.a1-pHCl-AGT lacking both the N-terminal helix and the M3-M4 loop could be expressed in Sf9 cells, and the receptor was targeted to membranes (supplemental Fig. 3). Both of them were resistant to solubilization with DDM but could be solubilized with a buffer containing 2% Fos-choline-12 instead of DDM. No functional study was done in oocytes.

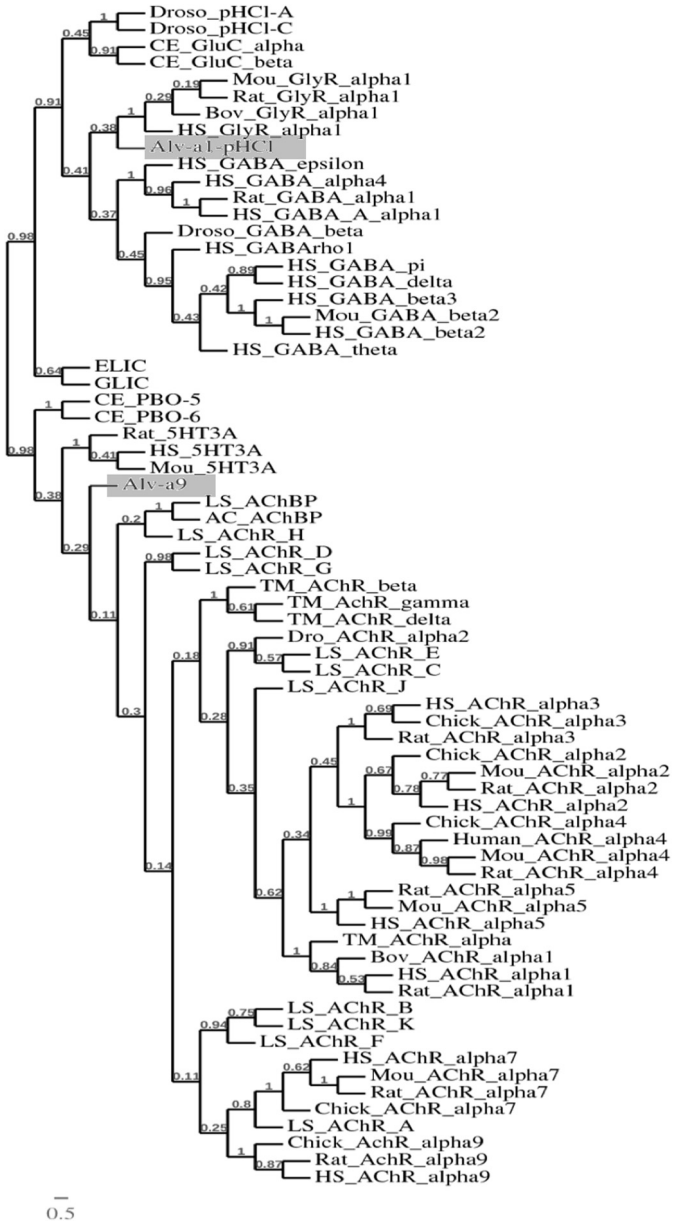


FIGURE 3. **Relationship with other members of the CLR family.** The dendrogram was constructed using a phylogenetic analysis platform. Alignment was done with MUSCLE (47) and phylogenetic analysis by PHYML (13, 45), with a statistical set of bootstrap values of 100 (46).

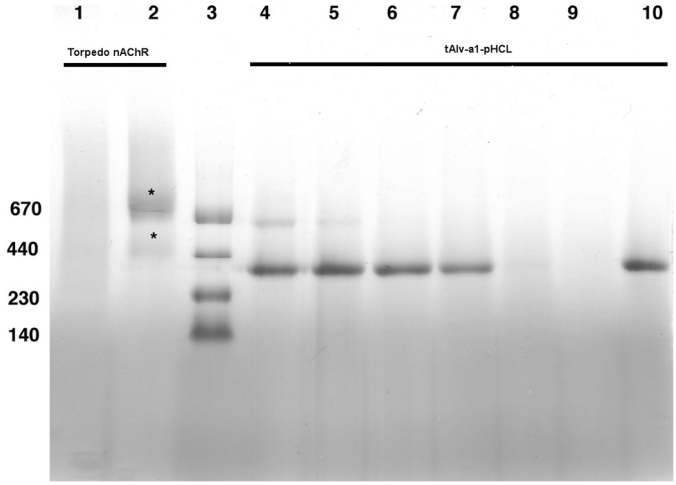


FIGURE 4. **Thermostability assay for tAlv-a1-pHCl and nAChR from *T. californica*.** The *Torpedo* receptor was affinity-purified in complex with bungarotoxin in the detergent Cymal6. The tAlv-a1-pHCl receptor was solubilized with DDM and purified as described above. *Torpedo* nAChR was incubated for 10 min at 50 °C (*lane 1*) and at room temperature (*lane 2*). Alv-a1-pHCl was incubated for 10 min at room temperature and at 40, 50, 55, 65, and 70 °C (*lanes 4–9*) and for 20 min at 50 °C (*lane 10*). The samples were applied to a blue native PAGE with a 18–4% acrylamide gradient. The marker proteins (*lane 3*) were at 670, 440, 230, and 140 kDa.

*Alv-a9*—The sequence homology observed between the $\alpha$9 nicotinic acetylcholine receptor and Alv-a9 suggests that this *Alvinella* gene might encode for a functional homopentameric ligand-gated channel. To probe the functionality of Alv-a9, oocyte experiments were conducted. Cells injected with the corresponding expression vector were tested with the same set of neurotransmitters as Alv-a1-phCl and with a sudden change to low pH. None of the cells displayed a significant inward or outward current different from control cells (data not shown).

## DISCUSSION

*Sequence Similarity and Phylogeny*—We report here two complete CLR gene sequences from the thermophilic eukaryotic annelid *A. pompejana*, Alv-a1-pHCl and Alv-a9. We were able to retrieve full-length sequences using overlapping sequence information from two EST databases. Alv-a1-pHCl shares 36% sequence identity with the human homopentameric $\alpha$1 glycine receptor. Alv-a9 shares 27% identity with the human homopentameric nAChR $\alpha$9 subunit. In comparison, the sequence of the prokaryotic CLR GLIC shares only 18–20% sequence identity with the latter. A sequence alignment of Alv-a1-pHCl and Alv-a9 with other CLRs is given in supplemental Fig. 1*A*.

In accord with these findings, a phylogenetic dendrogram groups Alv-a1-pHCl in one branch with anion-selective neuronal CLRs (Fig. 3), whereas the pH-sensitive, anion-selective CLRs from *Caenorhabditis elegans*, PBO-5 and PBO-6, are grouped into different branches of CLRs. Alv-a9 is grouped with cation-selective CLRs. Both Alv-a1-pHCl and Alv-a9 share characteristic structural features that are found in eukaryotic CLRs but absent in prokaryotic homologues, *i.e.* an N-terminal helix, the preserved Cys loop motif, and a CP mainly formed by a lengthy M3-M4 loop (Fig. 1, *A* and *B*, and supplemental Fig. 1*A*). These shared characteristics of *Alvinella* CLRs with other eukaryotic CLRs and the phylogenetic classification put *Alvinella* CLRs in a closer relationship with eukaryotic CLRs than with prokaryotic CLR homologues.

*pH Activation and Pharmacological Profile*—Expression of both *Alvinella* receptors, Alv-a1-pHCl and Alv-a9, was attempted in *Xenopus* oocytes. The neurotransmitters ACh, GABA, glutamate, and glycine did not evoke current (Fig. 5). A sudden change to low pH had no effect on Alv-a9, but in Alv-a1-pHCl, it evoked a typical current response. This was observed for Alv-a1-pHCl and tAlv-a1-pHCl (Fig. 5) but not for tAlv-a1-pHCl-AGT. The pH activation of tAlv-a1-pHCl showed an $EC_{50}$ at 3.24 with a Hill coefficient of 2.55 (Fig. 6). Chloride was found to be the major permeating ion (Fig. 7), in agreement with sequence patterns of M2 known to be charac-

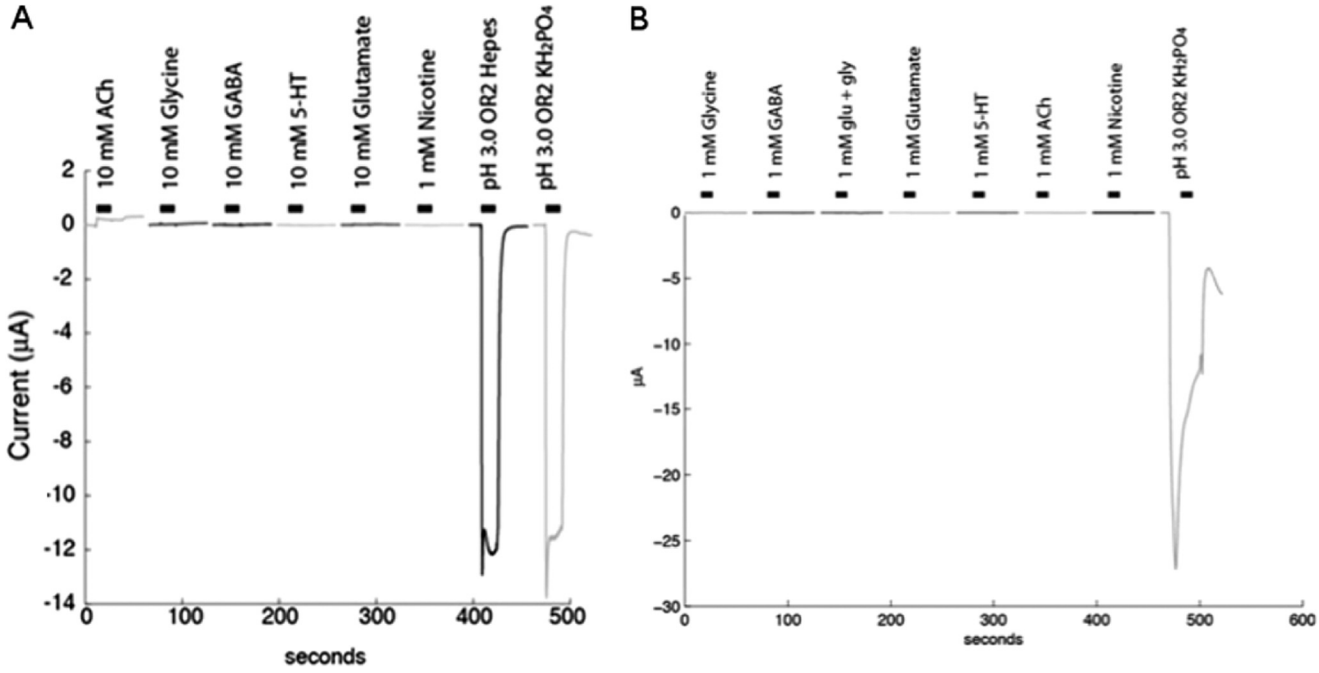


FIGURE 5. **Channel activity of Alv-a1-pHCl and tAlv-a1-pHCl observed in *Xenopus* oocytes.** *A*, tAlv-a1-pHCl was expressed in *Xenopus* oocytes, and activation was tested with different neurotransmitters (the concentrations tested are indicated). Robust inward currents were only evoked by lowering the pH. *B*, the same for Alv-a1-pHCl. Control experiments with non-expressing oocytes were conducted at pH 4.7 (47 oocytes) and pH 3.0 (66 oocytes) and yielded average currents of −0.12 and −0.40 $\mu$A with a standard error of 0.09 and 0.20, respectively.

teristic for anion-selective CLRs (21) (supplemental Fig. 1*B*) and the phylogenetic grouping of Alv-a1-pHCl with other anion-selective channels (Fig. 3). The 9′ Leu that is conserved in the M2 helix in most CLRs (22) is replaced by Met in Alv-a1-pHCl (Ile in GLIC) (supplemental Fig. 1*B*).

In comparison, the cation-selective homopentamer GLIC showed activation upon a pH drop with an $EC_{50}$ at pH 4.9 (7) or at pH 2.9 (23). The reported Hill coefficients varied between 1 and 2. Although, in oocytes, desensitization of GLIC was not observed (7), Velisetti *et al.* (23) reported single-exponential desensitization within several seconds after reconstitution into liposomes made of *Escherichia coli* polar lipids and addition of cholesterol further accelerated desensitization. The primary proton-binding event that promotes channel opening may take place in the known region of the binding site for other neurotransmitters, *i.e.* in the interface between adjacent subunits (2, 24, 25).

*Other pH-gated or pH-modulated Eukaryotic CLRs*—The *Drosophila* pHCl-A receptor forms homopentamers in oocytes. Upon raising the pH to above pH 7.3, Schnizler *et al.* (26) observed the onset of a chloride current with a pH response (Hill number 1.07) that did not desensitize as long as the pH was in the alkaline range. Temperature (in the range of 15–30 °C) is a positive modulator for the activation of these channels. That is, it raises the amplitude of the current. According to this work, the channels are modulated by ivermectin and desensitize on a time scale of tenths of seconds.

In *C. elegans*, Beg *et al.* (27) observed two CLR proteins, PBO-5 and PBO-6. Although oocytes after injection of PBO-6 mRNA show no response to typical neurotransmitters, there is a small activation seen upon a pH drop with PBO-5. Likewise, when PBO-5 and PBO-6 are coexpressed, there is no response to neurotransmitters but a distinct response to a pH drop with an $EC_{50}$ at approximately pH 6.8 and a Hill coefficient of 5. The sequences suggest that this is a cation-selective channel. This receptor is expressed in the posterior body muscles of the worm and seems to function in the periodic defecation.

*pH Activation Is Modulated by the N-terminal Residues*—In the presence of the N-terminal 37-residue extension (Alv-a1-pHCl), the pH 3.5-activated current changes its typical course when the pH is relaxing back to 7.4 by turning into a rebound current (Fig. 10), which is not seen in the truncated construct tAlv-pHCl. Rebound currents have been observed after the addition of agonists and various allosteric modulators (*e.g.* see Refs. 24, 28, 29). Wooltorton *et al.* (24) observed that phenobarbitone (PB) is an agonist for GABA $\beta$3 homopentamers, but, at higher concentrations, it is also blocking the current. Upon adding PB at high concentrations, a transient "smaller" current peak was seen, and this desensitized as usual. But when the oocytes were washed to bring the PB concentration down, a rebound current was observed. The authors propose that the usual transient activation current is occurring as long as only a few PB binding sites of the pentamer are occupied. As soon as more sites are occupied, the channel is in a stable desensitized state (no current), which cannot convert to a closed channel but only into an open channel.

When the PB concentration drops, these "sleeping" receptors "wake up" and undergo the activation and desensitization cycle indicated by the rebound current. In the spirit of this model, we offer an explanation for our observation. After the pH drop, five binding sites for the N-terminal extension in the LBDs are becoming exposed. As long as only a certain small fraction of the five extensions bind to the LBD sites, the receptor undergoes its normal activation cycle. However, in some

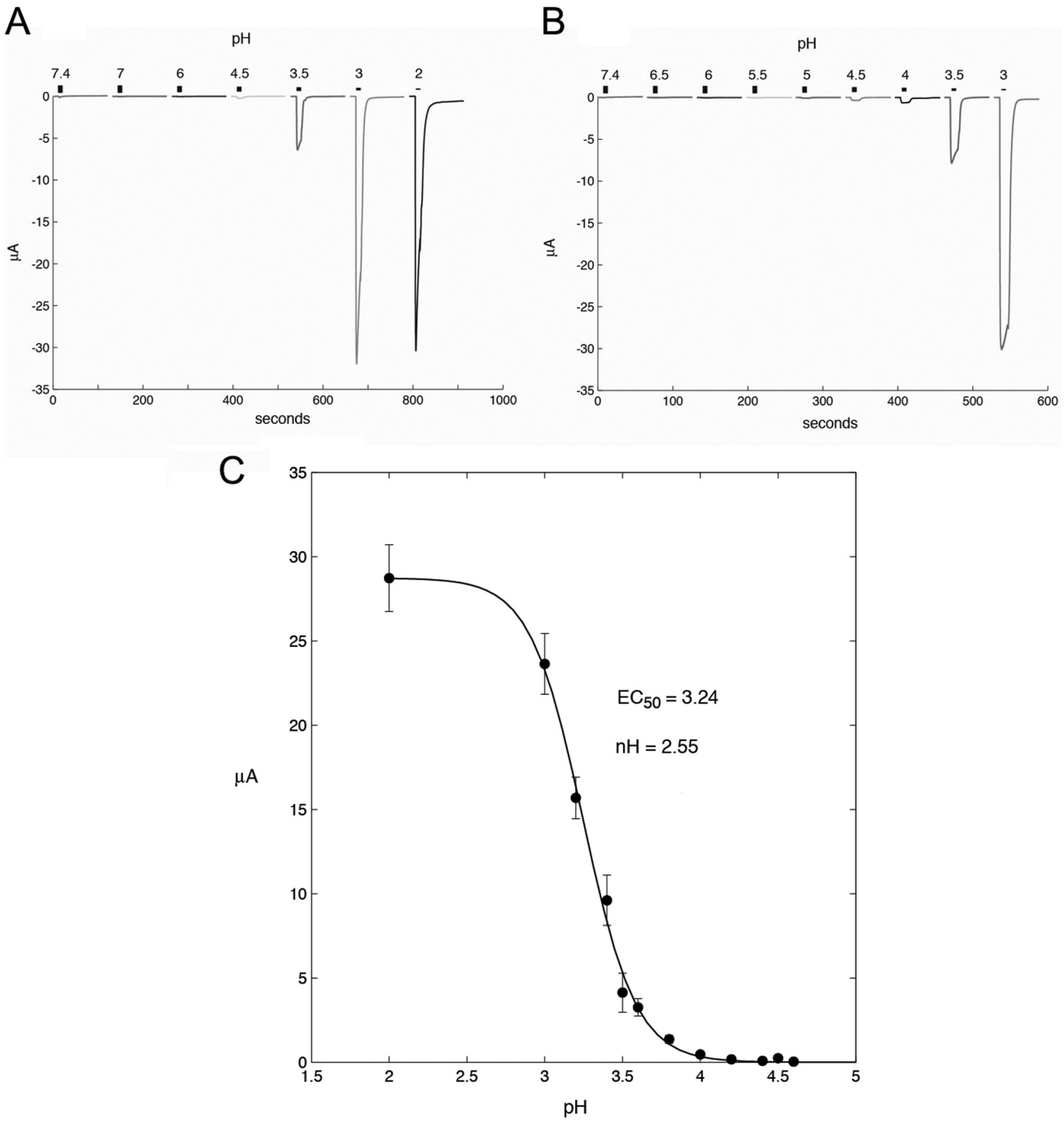


FIGURE 6. **Activation of tAlv-a1-pHCl by pH.** *A*, tAlv-a1-pHCl course pH screen. *B*, tAlv-a1-pHCl fine pH screen. *C*, pH induced channel activation was fitted with a Hill equation and yielded an $EC_{50}$ of 3.24 and a Hill coefficient of 2.5 for tAlv-a1-pHCl. *Error bars* indicate mean ± S.E. The currents measured at the indicated pH values are from between 4 and 14 oocytes.

receptors more than the critical number of the sites may be occupied by extensions. These receptors are stably desensitized. When the pH is raised back to 7, the extensions dissociate from the, and the receptors undergo activation, hence the rebound current.

*Sensitivity to Picrotoxin and Fipronil*—Both Alv-a1-pHCl and tAlv-a1-pHCl show similar weak and partial inhibition by picrotoxin (Fig. 8). In the structure of GluCl α (20), picrotoxin binds near the cytoplasmic mouth of the pore. The binding involves a −2′ Pro and a 2′ Thr on M2. Sequence alignment shows that the −2′ Pro is conserved in Alv-a1-pHCl as in all anion-selective channels (supplemental Fig. 1*B*). A Ser in Alv-a1-pHCl replaces the Thr, as in many other members of this family. tAlv-a1-pHCl is insensitive to fipronil, which is known as a very potent channel blocker of anionic receptors in invertebrates and vertebrates (30).

*Sensitivity to Ivermectin*—We observed that the pH-activated current of tAlv-a1-pHCl is insensitive to ivermectin. However, Alv-a1-pHCl, in addition to its rebound current, also showed a strong modulation in the presence of ivermectin (Fig.

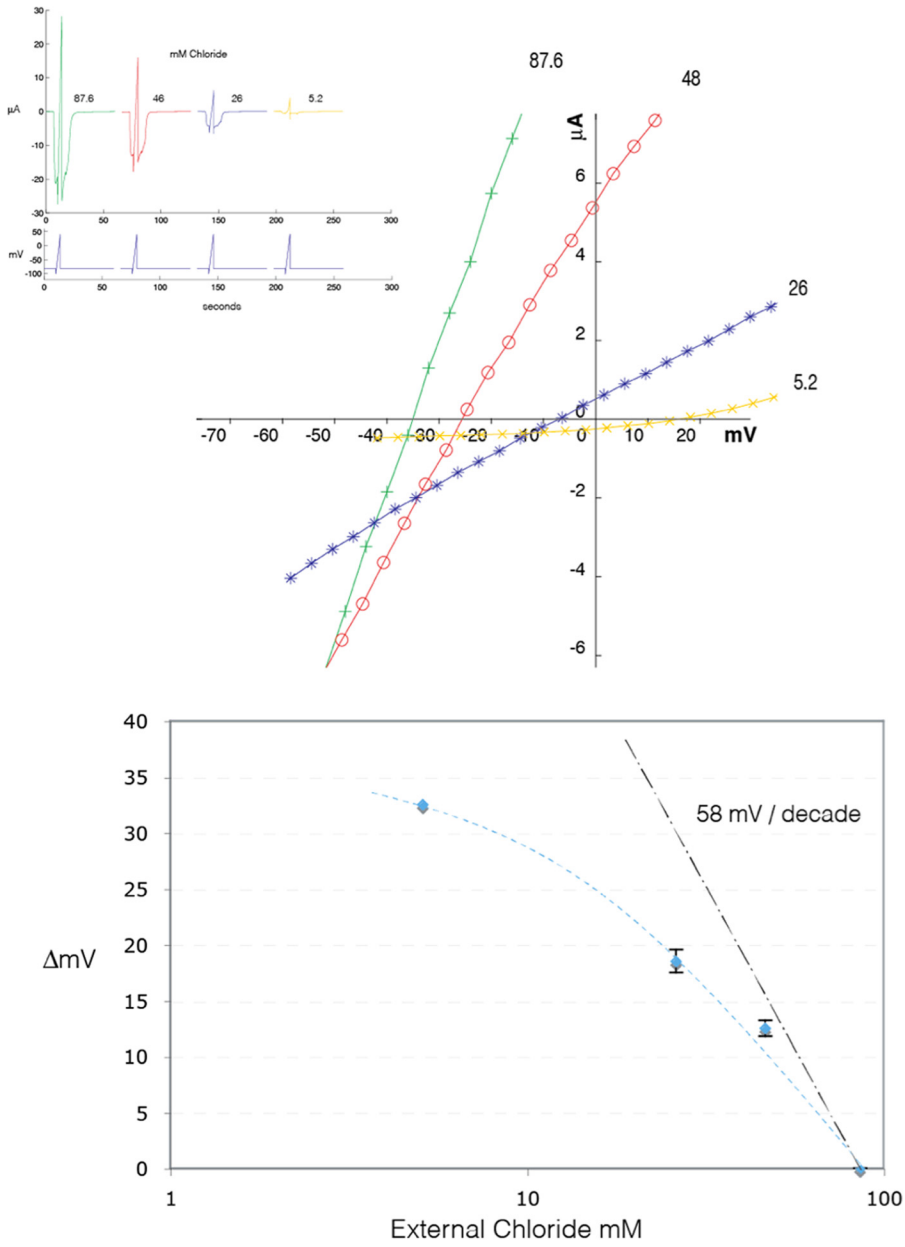


FIGURE 7. **tAlv-a1-pHCl is permeable to chloride ions.** The reversal potential for the pH-evoked current was determined by applying a voltage ramp protocol, illustrated by the *blue traces* in the *top panel*, first under control conditions (87.6 mM) and then in a series of decreasing extracellular concentrations of chloride. In these experiments, sodium chloride was replaced by mannitol. Reducing the extracellular chloride concentration caused both a reduction in the amplitude of the response, as seen on the current traces, and a shift of the reversal potential observed in the *center panel*. The plot of the shift of the reversal potential as a function of the logarithm of the extracellular chloride concentration reveals that the Alv-a1-pHCl receptors are permeable to chloride ions and display an ionic selectivity close to the 58 mV/decade predicted for a channel exclusively permeable to chloride ions. *Error bars* indicate mean ± S.E.

10). Because of the enhanced rebound effect with slowed desensitization, the binding of ivermectin apparently leads to a long-lived open channel conformation of Alv-a1-pHCl. Long-lived open channel conformations because of ivermectin were also observed for a human $\alpha/\beta$ glycine receptor in HEK cells after glycine application (31), for a nematode glutamate-gated chloride channel after glutamate application (32), and for a high-pH gated CLR from a parasitic mite after pH rise (33). The structure of GluCl $\alpha$ (20) shows ivermectin bound between transmembrane helices. The almost permanent opening may be due to a low $k_{off}$ rate for the dissociation of ivermectins from their sites in the helical interfaces.

Our observations suggest that ivermectin binding to the transmembrane helices of Alv-a1-pHCl may be enhanced when the extensions are bound to the LBDs. Indirect evidence for interactions of an N-terminal extension with its C-terminal CLR domain follows from the work of Ghosh *et al.* (34) on the GluCl-$\alpha$ CLR from *C. elegans*. These authors observed that the susceptibility for ivermectin is abrogated by deletions in a short, five-residue-long QQART motif ~35 residues upstream of the beginning of the N-terminal helix. This particular motif is, however, absent in Alv-a1-pHCl (Fig. 2*A*).

The physiologic result of ivermectin administration in parasitic nematodes may be inhibition of pharyngeal pumping by

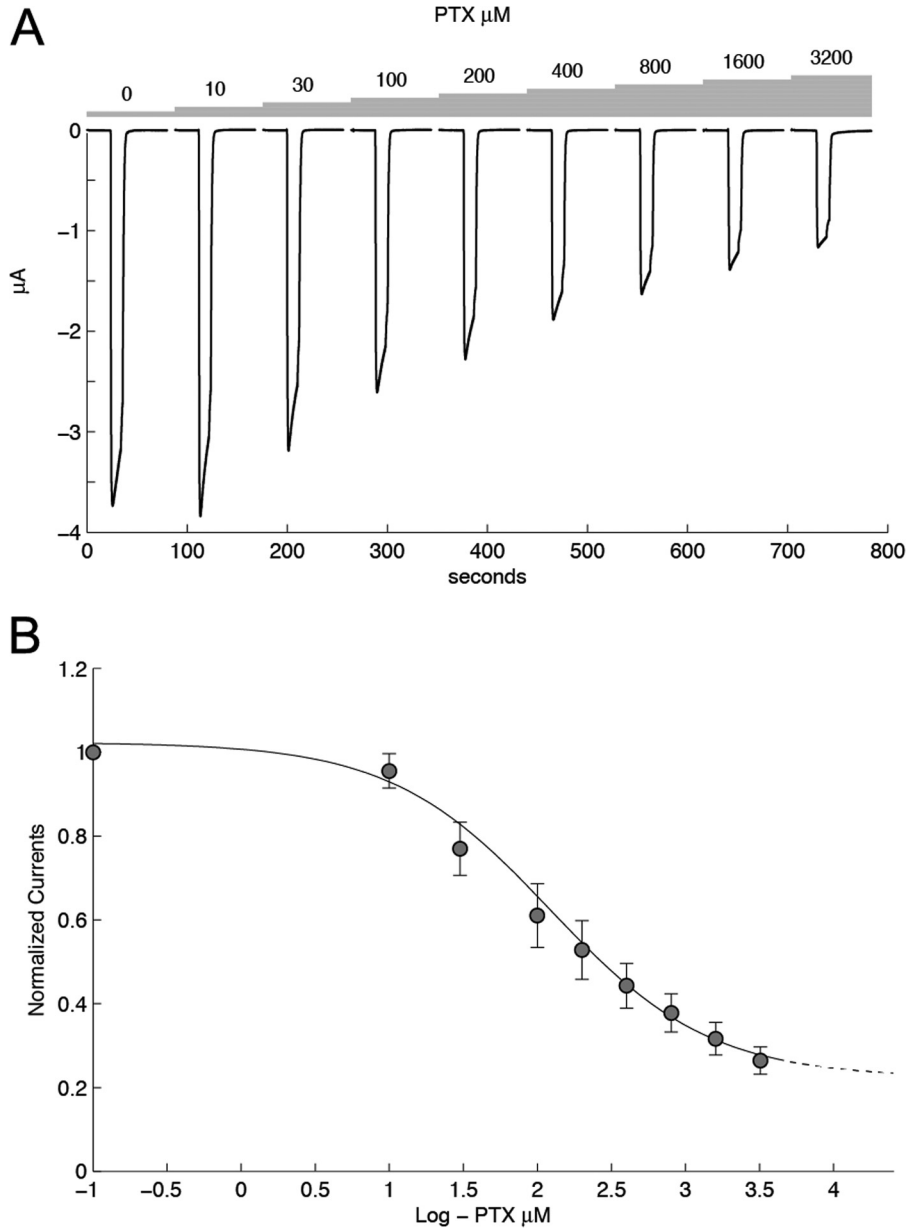


FIGURE 8. **tAlv-a1-pHCl is partially inhibited in the presence of picrotoxin.** *A*, data obtained from a single cell with exposure to different concentrations of picrotoxin (*PTX*) illustrates that these molecules partially inhibit the pH-evoked response. Cells were exposed for 10 s in the presence of picrotoxin before the pH jump (pH 3). *B*, plot of the current, normalized to unity, *versus* the response for picrotoxin recorded under control conditions yielded a dose-response curve that is fitted with a Hill equation with an $IC_{50}$ of 123 $\mu$M and a coefficient of 0.8. The data are from three oocytes. *Error bars* indicate mean ± S.E. Note that even at the highest concentration tested (3200 $\mu$M), picrotoxin only partially inhibits the pH-evoked current, and a constant of 0.22 was added.

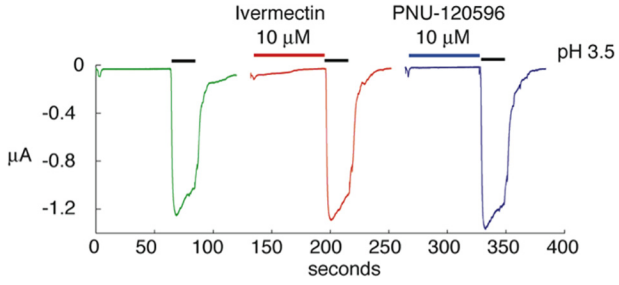


FIGURE 9. **tAlv-a1-pHCl is insensitive to the modulators ivermectin and PNU-120596.** Shown is the current after a pH drop from 7.5 to 3.5 (*black bar*). *Green*, without exposure; *red*, pre-exposure with 10 $\mu$M ivermectin; *blue*, pre-exposure with 10 $\mu$M PNU-120596.

coactivation of Glu-gated channels (34, 35). Because of sequence homology with the GluCl $\alpha$ channel from *C. elegans*, we speculate that Alv-a1-pHCl activation by low pH may also lead to the inhibition of pharyngeal pumping and may have a protective function for the *Alvinella* worm in case of a sudden acidification of the environment.

*Role of the N-terminal Helix and the M3-M4 Loop*—One feature of Alv-a1-pHCl is the N-terminal helix that is absent in a pH-sensitive prokaryotic homologue such as GLIC. To characterize its role, thAlv-a1-pHCl was constructed, which lacks the helix and was expressed in Sf9 cells. The receptor protein was targeted to membranes, as seen in a Western blot analysis with anti-His tag antibody (supplemental Fig. 3). From this mutant,

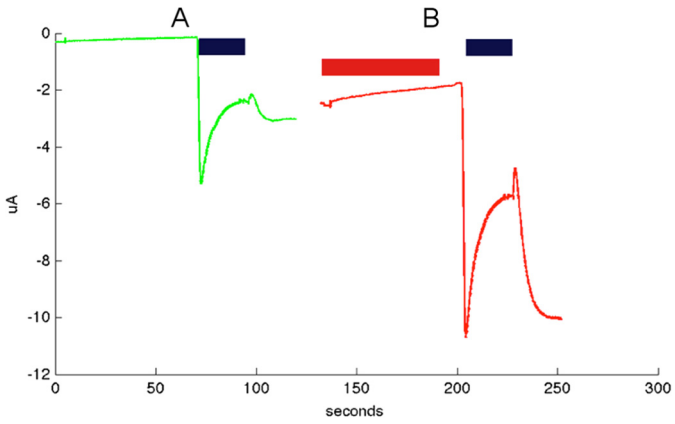


FIGURE 10. **Alv-a1-pHCl shows a rebound current upon activation and is coactivated by ivermectin.** *A*, *green*, current after a pH drop 7.5 to 3.5 (*black bar*). *B*, *red*, current from the same oocyte after ivermectin exposure (10 $\mu$M) for 60 s (*red bar*), washing, and a pH drop as above. This experiment was repeated with four different oocytes, yielding very similar currents.

thAlv-a1-pHCl-AGT was constructed, in which the M3-M4 loop was replaced by the tripeptide AGT. When expressed in Sf9 cells, the receptor was still found in the membrane fraction (supplemental Fig. 3), indicating that neither the N-terminal helix nor the M3-M4 loop are required for the biogenesis and targeting to membranes. Both proteins were resistant to solubilization with DDM but could be solubilized with 2% of the zwitterionic detergent Fos-choline-12. This could indicate that the N-terminal helix shields charges that, in its absence, are exposed and interact with another receptor LBD or with lipid head groups. The result with thAlv-a1-pHCl is in agreement with Bar-Lev *et al.* (36), who have shown that a similarly truncated $\alpha$7-GlucCl$\beta$ chimeric protein lacking the N-terminal helix is expressed even though it lacked ligand binding and response to the neurotransmitter.

It has been shown earlier that changes in the M3-M4 loop in eukaryotic CLRs alter expression and desensitization (37–39), modulate interaction with other proteins (40), and affect the single channel conductance in cation-selective CLRs (41). Alv-a1-pHCl has an intracellular M3-M4 loop that is 25–30 amino acids long. This is the shortest M3-M4 loop ever reported for eukaryotic CLRs, and it is rich in lysine and alanine (~20% each).

When the tAlv-a1-pHCl-AGT construct lacking the M3-M4 loop was expressed in oocytes, no current was observed. McKinnon *et al.* (37) have shown, for the 5-HT3A receptor, that mutants with a polyalanine sequence replacing the native M3-M4 loop were functional, disfavoring a role of charged residues in loss of function. In tAlv-a1-pHCl-AGT, it may be that replacing the M3-M4 loop with the tripeptide AGT restricts the conformational flexibility of the M3 and M4 helices. This may affect the conformations of the M2 helix, resulting in an inactive receptor, whereas a longer linker might lead to an active receptor.

*Thermostability*—On blue native PAGE, tAlv-a1-pHCl migrates with an apparent molecular weight of a pentamer. Thermostability was assayed by heat treatment of purified tAlv-a1-pHCl and blue native PAGE analysis (Fig. 4). The result suggests that the protein denatured after an incubation period of 10–20 min at a temperature between 55 and 65 °C. In comparison, the nAChR from *T. californica* in complex with $\alpha$-bungarotoxin denatured between 40 and 50 °C. This denaturation temperature of the *Alvinella* receptor, on the other hand, is not as high as expected for an organism that allegedly lives at temperatures as high as 80 °C (10, 11), conditions that are aggravated further by strong ambient temperature variations. The replacement of the membrane environment by a detergent micelle or other altered solvent conditions might have modulated the denaturation temperature. On the other hand, our results fit well to those from other *A. pompejana* proteins. A DNA polymerase (42) was stable after 5 min of incubation at 58 °C, exceeding the denaturation temperature of the human homologue by 21 °C. Collagen (43) was stable after heating to 45 °C, exceeding the denaturation temperature of shallow seawater annelids by 17 °C. Holder *et al.* (44) report further denaturation temperatures of a set of *A. pompejana* proteins that exceed their orthologues from mesophilic eukaryotic organisms by 4–8 °C.

*Alv-a9*—The failure to find a response after expressing this protein in oocytes could be due to several causes. The protein may not have been expressed because of inaptness of the assembly apparatus in oocytes or because Alv-a9 is one subunit of a hetero-oligomer. It is also possible that a pentameric homo-oligomer was expressed and that the correct agonist has not been applied or that the activation would occur only at temperatures above those used in the experiment. High temperature alone might even act as the agonist but cannot be applied to the oocytes.

*Acknowledgments—We thank Prof. Vladimir Katanaev for indicating the existence of the EST sequence database. We also thank Gabriele Maul for help with the construction of the Sf9 overexpression system in the laboratory of Prof. Hartmut Michel (Max Planck Institute for Biophysics, Frankfurt, Germany).*

## REFERENCES

1. Smart, T. G., and Paoletti, P. (2012) Synaptic neurotransmitter-gated receptors. *Cold Spring Harb. Perspect. Biol.* **4,** 1–26
2. Corringer, P.-J., Poitevin, F., Prevost, M. S., Sauguet, L., Delarue, M., and Changeux, J.-P. (2012) Structure and pharmacology of pentameric receptor channels: from bacteria to brain. *Structure* **20,** 941–956
3. Sine, S. M., and Engel, A. G. (2006) Recent advances in Cys-loop receptor structure and function. *Nature* **440,** 448–455
4. Miyazawa, A., Fujiyoshi, Y., and Unwin, N. (2003) Structure and gating mechanism of the acetylcholine receptor pore. *Nature* **423,** 949–955
5. Karlin, A. (2002) Emerging structure of the nicotinic acetylcholine receptors. *Nat. Rev. Neurosci.* **3,** 102–114
6. Tasneem, A., Iyer, L. M., Jakobsson, E., and Aravind, L. (2005) Identification of the prokaryotic ligand-gated ion channels and their implications for the mechanisms and origins of animal Cys-loop ion channels. *Genome Biol.* **6,** R4
7. Bocquet, N., Prado de Carvalho, L., Cartaud, J., Neyton, J., Le Poupon, C., Taly, A., Grutter, T., Changeux, J.-P., and Corringer, P.-J. (2007) A prokaryotic proton-gated ion channel from the nicotinic acetylcholine receptor family. *Nature* **445,** 116–119
8. Bocquet, N., Nury, H., Baaden, M., Le Poupon, C., Changeux, J.-P., Delarue, M., and Corringer, P.-J. (2009) X-ray structure of a pentameric ligand-gated ion channel in an apparently open conformation. *Nature* **457,** 111–114
9. Desbruyères, D., and Laubier, L. (1980) *Alvinella pompejana* gen. sp. nov., aberrant Ampharetidae from the East Pacific Rise hydrothermal vents.

*Oceanologica Acta* **3,** 267–274
10. Stein, S. T., and Cary, S. C. (1998) Worm bask in extreme temperatures. *Nature* **391,** 545–546
11. Le Bris, N., and Gaill, F. (2006) How does the annelid *Alvinella pompejana* deal with an extreme hydrothermal environment? *Rev. Environ. Sci. Biotechnol.* **6,** 197–221
12. Gagnière, N., Jollivet, D., Boutet, I., Brélivet, Y., Busso, D., Da Silva, C., Gaill, F., Higuet, D., Hourdez, S., Knoops, B., Lallier, F., Leize-Wagner, E., Mary, J., Moras, D., Perrodou, E., Rees, J.-F., Segurens, B., Shillito, B., Tanguy, A., Thierry, J.-C., Weissenbach, J., Wincker, P., Zal, F., Poch, O., and Lecompte, O. (2010) Insights into metazoan evolution from *Alvinella pompejana* cDNAs. *BMC Genomics* **11,** 634
13. Dereeper, A., Guignon, V., Blanc, G., Audic, S., Buffet, S., Chevenet, F., Dufayard, J.-F., Guindon, S., Lefort, V., Lescot, M., Claverie, J.-M., and Gascuel, O. (2008) Phylogeny.fr: robust phylogenetic analysis for the non-specialist. *Nucleic Acids Res.* **36,** W465–469
14. Heuberger, E. H., Veenhoff, L. M., Duurkens, R. H., Friesen, R. H., and Poolman, B. (2002) Oligomeric state of membrane transport proteins analyzed with blue native electrophoresis and analytical ultracentrifugation. *J. Mol. Biol.* **317,** 591–600
15. Hoda, J.-C., Gu, W., Friedli, M., Phillips, H. A., Bertrand, S., Antonarakis, S. E., Goudie, D., Roberts, R., Scheffer, I. E., Marini, C., Patel, J., Berkovic, S. F., Mulley, J. C., Steinlein, O. K., and Bertrand, D. (2008) Human nocturnal frontal lobe epilepsy: pharmocogenomic profiles of pathogenic nicotinic acetylcholine receptor $\beta$-subunit mutations outside the ion channel pore. *Mol. Pharmacol.* **74,** 379–391
16. Hogg, R. C., Bandelier, F., Benoit, A., Dosch, R., and Bertrand, D. (2008) An automated system for intracellular and intranuclear injection. *J. Neurosci. Methods* **169,** 65–75
17. Silberberg, S. D., Li, M., and Swartz, K. J. (2007) Ivermectin interaction with transmembrane helices reveals widespread rearrangements during opening of P2X receptor channels. *Neuron* **54,** 263–274
18. Krause, R. M., Buisson, B., Bertrand, S., Corringer, P. J., Galzi, J. L., Changeux, J. P., and Bertrand, D. (1998) Ivermectin: a positive allosteric effector of the $\alpha$7 neuronal nicotinic acetylcholine receptor. *Mol. Pharmacol.* **53,** 283–294
19. Hurst, R. S., Hajós, M., Raggenbass, M., Wall, T. M., Higdon, N. R., Lawson, J. A., Rutherford-Root, K. L., Berkenpas, M. B., Hoffmann, W. E., Piotrowski, D. W., Groppi, V. E., Allaman, G., Ogier, R., Bertrand, S., Bertrand, D., and Arneric, S. P. (2005) A novel positive allosteric modulator of the $\alpha$7 neuronal nicotinic acetylcholine receptor: *in vitro* and *in vivo* characterization. *J. Neurosci.* **25,** 4396–4405
20. Hibbs, R. E., and Gouaux, E. (2011) Principles of activation and permeation in an anion-selective Cys-loop receptor. *Nature* **474,** 54–60
21. Jensen, M. L., Schousboe, A., and Ahring, P. K. (2005) Charge selectivity of the Cys-loop family of ligand-gated ion channels. *J. Neurochem.* **92,** 217–225
22. Thompson, A. J., Alqazzaz, M., Ulens, C., and Lummis, S. C. (2012) The pharmacological profile of ELIC, a prokaryotic GABA-gated receptor. *Neuropharmacology* **63,** 761–767
23. Velisetty, P., and Chakrapani, S. (2012) Desensitization mechanism in prokaryotic ligand-gated ion channel. *J. Biol. Chem.* **287,** 18467–18477
24. Duret, G., Van Renterghem, C., Weng, Y., Prevost, M., Moraga-Cid, G., Huon, C., Sonner, J. M., and Corringer, P.-J. (2011) Functional prokaryotic-eukaryotic chimera from the pentameric ligand-gated ion channel family. *Proc. Natl. Acad. Sci. U.S.A.* **108,** 12143–12148
25. Celie, P. H., van Rossum-Fikkert, S. E., van Dijk, W. J., Brejc, K., Smit, A. B., and Sixma, T. K. (2004) Nicotine and carbamylcholine binding to nicotinic acetylcholine receptors as studied in AChBP crystal structures. *Neuron* **41,** 907–914
26. Schnizler, K., Saeger, B., Pfeffer, C., Gerbaulet, A., Ebbinghaus-Kintscher, U., Methfessel, C., Franken, E.-M., Raming, K., Wetzel, C. H., Saras, A., Pusch, H., Hatt, H., and Gisselmann, G. (2005) A novel chloride channel in *Drosophila melanogaster* is inhibited by protons. *J. Biol. Chem.* **280,** 16254–16262
27. Beg, A. A., Ernstrom, G. G., Nix, P., Davis, M. W., and Jorgensen, E. M. (2008) Protons act as a transmitter for muscle contraction in *C. elegans*. *Cell* **132,** 149–160
28. Wooltorton, J. R., Moss, S. J., and Smart, T. G. (1997) Pharmacological and physiological characterization of murine homomeric $\beta$3 GABA(A) receptors. *Eur. J. Neurosci.* **9,** 2225–2235
29. Papke, R. L., Kem, W. R., Soti, F., López-Hernández, G. Y., and Horenstein, N. A. (2009) Activation and desensitization of nicotinic $\alpha$7-type acetylcholine receptors by benzylidene anabaseines and nicotine. *J. Pharmacol. Exp. Ther.* **329,** 791–807
30. Gondhalekar, A. D., and Scharf, M. E. (2012) Mechanisms underlying fipronil resistance in a multiresistant field strain of the German cockroach (Blattodea: Blattellidae). *J. Med. Entomol.* **49,** 122–131
31. Shan, Q., Haddrill, J. L., and Lynch, J. W. (2001) Ivermectin, an unconventional agonist of the glycine receptor chloride channel. *J. Biol. Chem.* **276,** 12556–12564
32. McCavera, S., Rogers, A. T., Yates, D. M., Woods, D. J., and Wolstenholme, A. J. (2009) An ivermectin-sensitive glutamate-gated chloride channel from the parasitic nematode *Haemonchus contortus*. *Mol. Pharmacol.* **75,** 1347–1355
33. Mounsey, K. E., Dent, J. A., Holt, D. C., McCarthy, J., Currie, B. J., and Walton, S. F. (2007) Molecular characterisation of a pH-gated chloride channel from *Sarcoptes scabiei*. *Invert. Neurosci.* **7,** 149–156
34. Brownlee, D. J., Holden-Dye, L., and Walker, R. J. (1997) Actions of the anthelmintic ivermectin on the pharyngeal muscle of the parasitic nematode, *Ascaris suum*. *Parasitology* **115,** 553–561
35. Wolstenholme, A. J., and Rogers, A. T. (2005) Glutamate-gated chloride channels and the mode of action of the avermectin/milbemycin anthelmintics. *Parasitology* **131,** S85–95
36. Bar-Lev, D. D., Degani-Katzav, N., Perelman, A., and Paas, Y. (2011) Molecular dissection of Cl-selective Cys-loop receptor points to components that are dispensable or essential for channel activity. *J. Biol. Chem.* **286,** 43830–43841
37. McKinnon, N. K., Bali, M., and Akabas, M. H. (2012) Length and amino acid sequence of peptides substituted for the 5-HT3A receptor M3M4 loop may affect channel expression and desensitization. *PloS ONE* **7,** e35563
38. Hu, X.-Q., Sun, H., Peoples, R. W., Hong, R., and Zhang, L. (2006) An interaction involving an arginine residue in the cytoplasmic domain of the 5-HT3A receptor contributes to receptor desensitization mechanism. *J. Biol. Chem.* **281,** 21781–21788
39. O'Toole, K. K., and Jenkins, A. (2011) Discrete M3-M4 intracellular loop subdomains control specific aspects of $\gamma$-aminobutyric acid type A receptor function. *J. Biol. Chem.* **286,** 37990–37999
40. Millar, N. S. (2008) RIC-3: a nicotinic acetylcholine receptor chaperone: RIC-3: a nicotinic receptor chaperone. *Br. J. Pharmacol.* **153,** S177–S183
41. Kelley, S. P., Dunlop, J. I., Kirkness, E. F., Lambert, J. J., and Peters, J. A. (2003) A cytoplasmic region determines single-channel conductance in 5-HT3 receptors. *Nature* **424,** 321–324
42. Kashiwagi, S., Kuraoka, I., Fujiwara, Y., Hitomi, K., Cheng, Q. J., Fuss, J. O., Shin, D. S., Masutani, C., Tainer, J. A., Hanaoka, F., and Iwai, S. (2010) Characterization of a Y-family DNA polymerase eta from the eukaryotic thermophile *Alvinella pompejana*. *J. Nucleic Acids* 10.4061/2010/701472
43. Gaill, F., Mann, K., Wiedemann, H., Engel, J., and Timpl, R. (1995) Structural comparison of cuticle and interstitial collagens from annelids living in shallow sea-water and at deep-sea hydrothermal vents. *J. Mol. Biol.* **246,** 284–294
44. Holder, T., Basquin, C., Ebert, J., Randel, N., Jollivet, D., Conti, E., Jékely, G., and Bono, F. (2013) Deep transcriptome-sequencing and proteome analysis of the hydrothermal vent annelid *Alvinella pompejana* identifies the CvP-bias as a robust measure of eukaryotic thermostability. *Biol. Direct* **8,** 2
45. Guindon, S., Dufayard, J.-F., Lefort, V., Anisimova, M., Hordijk, W., and Gascuel, O. (2010) New algorithms and methods to estimate maximum-likelihood phylogenies: assessing the performance of PhyML 3.0. *Syst. Biol.* **59,** 307–321
46. Anisimova, M., and Gascuel, O. (2006) Approximate likelihood-ratio test for branches: a fast, accurate, and powerful alternative. *Syst. Biol.* **55,** 539–552
47. Edgar, R. C. (2004) MUSCLE: multiple sequence alignment with high accuracy and high throughput. *Nucleic Acids Res.* **19,** 1792–1797